Detection of the Linear Carbon Cluster C_{10}: Rotationally Resolved Diode-Laser Spectroscopy

Thomas F. Giesen,*[a] Ute Berndt,[a] Koichi M. T. Yamada,[a] Guido Fuchs,[a] Rudolf Schieder,[a] Gisbert Winnewisser,[a] Robert A. Provencal,[b] Frank N. Keutsch,[b] Alan Van Orden,[b] and Richard J. Saykally[b]

KEYWORDS:

carbon clusters · C_{10} · rotational spectroscopy · vibrational spectroscopy

The molecular structure of carbon clusters and their formation processes are of increasing interest ever since the discovery of the magic number cluster C_{60} in 1985 by Kroto et al.[1] This continued attention to research on carbon clusters stems from the fact that answers to some fundamental and long-standing problems in astrophysics and other fields of molecular physics can be found, once the detailed spectroscopic properties are understood. The importance and different roles of the carbon bonding in areas as diverse as astrophysics, reaction kinetics of combustion processes, and in molecular physics are now more appreciated. Spectroscopic studies with the aim of deriving the structures of carbon clusters have commenced.[2, 3] Remarkable progress has been made in recent years in both theoretical interpretation and experimental techniques in producing and sensitively measuring the different carbon clusters. For cluster sizes up to 20 carbon atoms, ab initio calculations predict two structures to be most stable, a linear form for small clusters and a cyclic form for the larger ones.

The linear isomers of odd-numbered $C_3 - C_{21}$ and of even-numbered $C_4 - C_{14}$ have been identified by their electronic spectra in neon matrices,[4–6] and recently C_5 in the gas phase.[7] Infrared-active vibrational bands have been observed for linear $C_3 - C_{12}$ and cyclic C_6 and C_8 in rare-gas matrices.[8–10] Among them, the IR spectra of linear $C_3 - C_7$, C_9, and C_{13} have been recorded in the gas phase with high resolution and the rotational fine structures have been analyzed.[3]

[a] *Dr. T. F. Giesen, Dr. U. Berndt, Dr. K. M. T. Yamada,[+] G. Fuchs, Prof. Dr. R. Schieder, Prof. Dr. G. Winnewisser*
I. Physikalisches Institut
Universität zu Köln, 50937 Köln (Germany)
Fax: (+49) 221-470-6152
E-mail: giesen@ph1.uni-koeln.de

[b] *Dr. R. A. Provencal, F. N. Keutsch, Dr. A. Van Orden,[++] Prof. Dr. R. J. Saykally[+]*
Department of Chemistry
University of California
Berkeley, CA 94720 (USA)

[+] *Current address:*
NIRE Tsukuba, Ibaraki 305-8569 (Japan)

[++] *Current address:*
Department of Chemistry
Colorado State University
Fort Collins, CO (USA)

[+] *R. J. Saykally is a member of the Editorial Advisory Board for ChemPhysChem.*

The electronic ground states of odd-numbered linear carbon clusters so far found are $^1\Sigma_g^+$, whereas for even-numbered clusters they are $^3\Sigma_g^-$. It should be noted, however, that little is known about the triplet character of even-numbered clusters. The ESR spectra of C_4,[11] C_6, and C_8 in solid rare-gas matrices published by Graham et al. and Van Zee et al. show an increase of the spin – spin coupling constant with increasing length of the carbon chain.[12] The ESR data assigned to C_{10} by these authors were found to be incorrect and due to unknown paramagnetic species other than pure carbon clusters,[12] as cited later by Endo and co-workers.[13] In the electronic spectra of $C_4 - C_{14}$ the triplet splitting remains unresolved.

The polycarbon monoxides, C_nO with $n = 1, 2, 3,\ldots$, are electronically the closest references for pure carbon clusters. Due to their nonzero permanent dipole moment, C_nO species can be studied in detail by pure rotational spectroscopy with very high spectral resolution, and the electronic ground state can be determined precisely. Endo and co-workers have measured the pure rotational spectra of $^3\Sigma$ linear C_4O, C_6O, and C_8O with Fourier-transform microwave spectroscopy with high spectral resolution and the $^1\Sigma$ state molecules C_5O, C_7O, and C_9O as well.[13, 14] They observed the fine structure of the $^3\Sigma$ state molecules and reported a significant increase of the spin – spin coupling constant with increasing chain lengths, in a good agreement with the ESR observations of $C_4O - C_6O$.[15]

Due to the zero permanent dipole moment of pure carbon clusters, no pure rotational spectra can be observed. They can, however, be studied by rotationally resolved IR spectroscopy, which in some cases allows a detailed analysis of the molecular fine structure. The triplet splittings of C_4 in the gas-phase IR spectra were found to be too small to be resolved in the Doppler limit,[11, 16, 17] but the IR spectrum of C_6 shows a partly resolved triplet splitting for the four lowest *P*- and *R*-branch transitions.[18] Since the spin – spin coupling increases with the number of carbon atoms, it should be resolved in the IR spectra of even-numbered C_n with *n* larger than 6.

In this paper, we present the first high-resolution gas phase rovibrational spectrum of linear C_{10} ever obtained, recorded with a tunable diode-laser spectrometer. The resolving power of 10^{-4} is sufficient to clearly separate the $^3\Sigma$ electronic spin splitting of the spectra. The observed large splittings in the rovibrational transitions of the (ν_6) asymmetric stretching band around 2074 cm^{-1} allowed us to assign the electronic ground state of C_{10} to be $^3\Sigma$. Figure 1 presents an overview of the gas-phase IR spectrum.

$^3\Sigma$ State in the Case (a) Limit

The effective spin-rotational Hamiltonian matrix $\boldsymbol{H}_{SR}$ for a $^3\Sigma$ electronic state is expressed by Equation (1),[23] where the first

$$\boldsymbol{H}_{SR} = B_v\boldsymbol{N}^2 - D_v\boldsymbol{N}^4 + \frac{2}{3}\lambda_v\left(3\boldsymbol{S}_z^2 - \boldsymbol{S}^2\right) + \gamma_v\boldsymbol{NS} \quad (1)$$

two terms account for the rotational energy in the vibrational state ν with rotational and centrifugal distortion constants *B* and *D*, the third term represents the spin – spin interaction with the interaction constant λ_v, and the last term signifies the spin – rotation interaction energy with constant γ_v.

  1439-4235/01/02/04 $ 17.50+.50/0 CHEMPHYSCHEM **2001**, No. 4

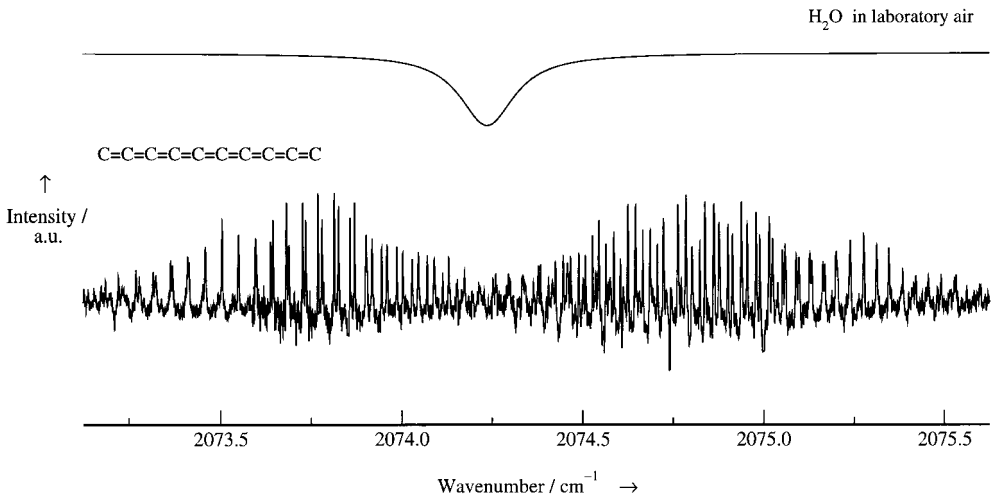

Figure 1. *The overview spectrum of C_{10} observed in the present study. The atmospheric water absorption reproduced in the upper trace hindered the measurements near the band center region.*

The energy matrix for a given total angular momentum quantum number $J \neq 0$ (that is, $\boldsymbol{J} = \boldsymbol{N} + \boldsymbol{S}$ in the present case) is calculated by Equation (2), where N is the rotational quantum number, and a, b, c, and d are given by Equations (3) – (6).

$$\begin{array}{ll} N = J-1 & \begin{pmatrix} a & 0 & d \\ 0 & b & 0 \\ d & 0 & c \end{pmatrix} \\ N = J & \\ N = J+1 & \end{array} \tag{2}$$

$$a = BJ(J-1) - DJ^2(J-1)^2 + \gamma(J-1) + \left(\frac{2}{3} - \frac{2J}{2J+1}\right)\lambda \tag{3}$$

$$b = BJ(J+1) - DJ^2(J+1)^2 - \gamma + \frac{2}{3}\lambda \tag{4}$$

$$c = B(J+1)(J+2) - D(J+1)^2(J+2)^2 + \gamma(J+2) + \left(\frac{2}{3} - \frac{2(J+1)}{2J+1}\right)\lambda \tag{5}$$

$$d = 2\frac{\sqrt{J(J+1)}}{2J+1}\lambda \tag{6}$$

The $J = 0$ state is composed only from the $N = 1$, that is $N = J + 1$, and the energy is given simply by c with $J = 0$.

If $|\lambda| \ll 4BJ$, the resulting energy eigenvalues are well expressed by Hund's case (b) limit, which leads to a narrowly spaced triplet structure denoted here conventionally by the terms F_1 for $N = J - 1$, F_2 for $N = J$, and F_3 for $N = J + 1$. The F_2 level is not mixed with the other two, and the F_1 and F_3 levels are, on the contrary, mixed slightly each other by the spin – spin interaction term of λ through the matrix element d. In this case, it should be noted that those three levels of the same J do not form the closely separated triplet. Instead, the levels of the same N compose the triplet; N is the good quantum number.

This picture, however, does not represent the case of C_{10}, a heavy, long carbon chain molecule very well. The rotational constant B of the C_{10} molecule is very small compared with the spin – spin interaction constant λ. In the case $|\lambda| \gg 4BJ$, the wavefunctions of F_1 and F_3 are strongly mixed and the eigenvalues of the energy matrix given above approach those of Hund's case (a) limit, which are usually denoted by $^3\Sigma_0$ and $^3\Sigma_1$ in the case (a) notation of $^{2S+1}\Lambda_{|\Omega|}$.

In order to understand the case (a) character of the $^3\Sigma$ state, it may be useful to derive the approximate eigenvalues of the energy matrix; ignoring all terms except for those of λ we obtain the result given by Equations (7) and (8).

$$\varepsilon(F_2) = \frac{2}{3}\lambda \tag{7}$$

$$\varepsilon(F_\pm) = -\frac{1}{3}\lambda \pm |\lambda| \tag{8}$$

The F_2 [Eq. (7)] represents the unmixed state of $N = J$, and the $F_\pm$ [Eq. (8)] are the mixed states of F_1 and F_3, where N is no longer a good quantum number. If $\lambda > 0$, we obtain Equations (9) and (10).

$$\varepsilon(F_+) = \frac{2}{3}\lambda \tag{9}$$

$$\varepsilon(F_-) = -\frac{4}{3}\lambda \tag{10}$$

The energy level of F_+ [Eq. (9)] is then degenerate with that of F_2 [Eq. (7)]. They represent the doubly degenerate $^3\Sigma_1$ state. The F_- energy [Eq. (10)] is identical to that of $J = 0$ within the approximation and they are of the nondegenerate $^3\Sigma_0$ state. Here the energy of the $^3\Sigma_0$ is lower than that of $^3\Sigma_1$; the splitting is *regular*.

On the contrary, if $\lambda < 0$, we obtain Equations (11) and (12).

$$\varepsilon(F_+) = -\frac{4}{3}\lambda \tag{11}$$

$$\varepsilon(F_-) = \frac{2}{3}\lambda \tag{12}$$

The energy level of F_- [Eq. (12)] is now degenerate with that of F_2 [Eq. (7)], to form the doubly degenerate $^3\Sigma_1$ state. The F_+ [Eq. (11)] together with the $J = 0$ are of the nondegenerate $^3\Sigma_0$ state. In this case the energy of the $^3\Sigma_0$ is higher than that of $^3\Sigma_1$; the splitting is *inverted*.

In the case where λ is large as in the present case, N is no more a good quantum number except for the levels of $N = J$. It is more convenient and suitable to use the case (a) quantum numbers J and Ω.

Figure 2 shows the schematic energy level diagrams of the $^3\Sigma$ state in the inverse case (a) limit. The doubly degenerate $|\Omega| = 1$ levels are split also in the case (a) limit; by the case (a) nomenclature, the splitting is called Λ-type doubling (more correctly it should be "Ω-type doubling" because Λ vanishes for a Σ electronic state). The two components of $|\Omega| = 1$ are distinguished by e and f.[24]

A more detailed discussion of the case (a) character of the $^3\Sigma$ state can be followed in the article published by Tatum and Watson.[25]

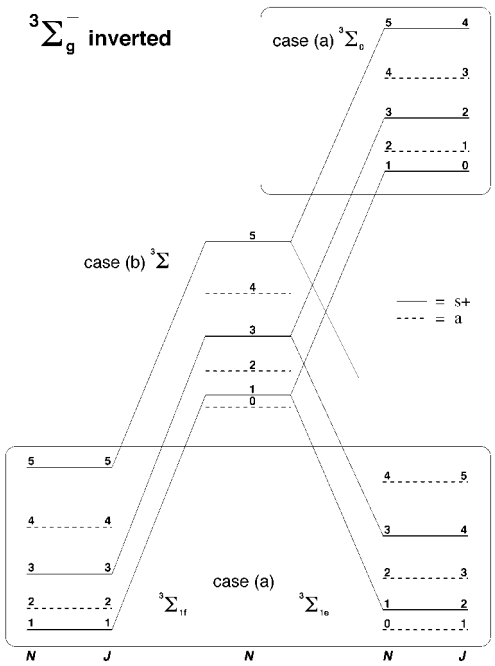

Figure 2. *Energy level diagram of C_{10}. Levels forbidden by nuclear-spin statistics are indicated by broken lines.*

Analysis and Results

Figure 3 shows the observed spectrum between 2073.0 – 2075.6 cm^{-1}. We have identified 134 rotationally resolved *R*- and *P*-branch transitions of a centrosymmetric linear molecule with a band origin at 2074.4 cm^{-1}.

The observed lines exhibit mainly two *R*-branches and two *P*-branches of a linear molecule. Due to the zero nuclear spin of carbon, Bose nuclear spin statistics are relevant and every other *J*-rotational line is missing in the spectrum of a molecule with $D_{\infty h}$ symmetry. We assigned one band to the even-numbered *J* rotational quantum numbers and the other band to the odd-numbered *J*. Since the electronic ground state of linear C_{10} is most likely a $^3\Sigma_g^-$ state, we assumed that the appearance of the two bands originates from a strong spin – spin coupling of the two unpaired electrons. Near the band center region, the lines appear alternatively and their apparent spacing is close to 2*B*. In the high-*J* regions, namely near 2073.6 cm^{-1} for the *P*-branch and 2075.3 cm^{-1} for the *R*-branch, the two components overlap and the apparent spacing of the rotational structure is close to 4*B*.

We have thus adjusted the parameters of the effective Hamiltonian, Equation (13), in order to reproduce the observed line positions by a least-squares fit procedure, where *G* represents the vibrational energy and $\boldsymbol{H}_{SR}$ is the effective rotational Hamiltonian of a $^3\Sigma$ state described in the previous section.

$$\boldsymbol{H} = G + \boldsymbol{H}_{SR} \tag{13}$$

The lines of the third component, $^3\Sigma_0$, have not been included in the preliminary fit; only G', B', B'', λ', and λ'' were adjusted. The best fit has been achieved by assigning the two sets of lines to the $^3\Sigma_1$ components of the inverted triplet states. Due to spin statistics alternate components of the doublet are missing. From the observed spectra we predict the temperature in the molecular C_{10} beam to be about 10 K.

In the high-*J* part of the *R*-branch (2075 cm^{-1}), several single lines have been identified very close to the line positions for the so far missing $^3\Sigma_0$ band, as predicted from the preliminary fit. After several trial-and-error iterations, we finally assigned these lines to the $^3\Sigma_0$ band. Most of the lines are overlapped by the $^3\Sigma_1$ lines, which are relatively strong at this temperature due to the favorable Boltzmann factor in the inverted case, especially in in the *P*-branch region. In addition, near the band center region, where the $^3\Sigma_0$ lines are predicted to be strong, the measurement is hindered strongly by atmospheric water absorption. Therefore, it was not easy to identify the *J* quantum number for the $^3\Sigma_0$ lines.

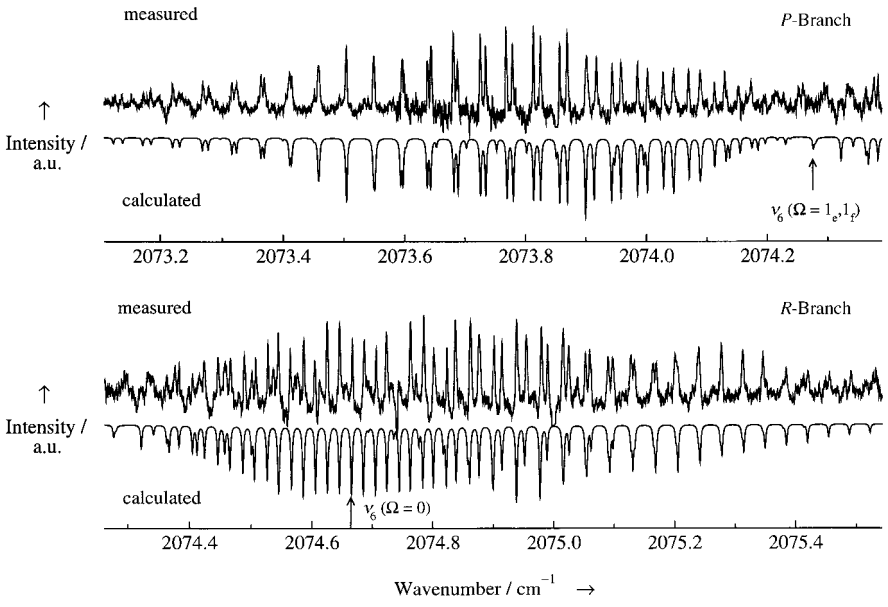

Figure 3. *Observed spectrum of linear C_{10} at roughly 10 K (upper trace) and, from the parameters of Table 4, calculated spectrum (lower trace). The band origins of the $^3\Sigma_1$ and $^3\Sigma_0$ bands are indicated by arrows.*

The simulated spectrum, obtained on the basis of the best-fit molecular constants, shows an excellent agreement with the observed one, as shown in Figure 3. The intensity of each transition is calculated from the formula for a intermediate coupling case given by Tatum and Watson (see Table 2).[25]

In Figure 4, the calculated spectra are shown in a stick diagram and the high frequency part of the observed spectra is shown together with the assignment.

Tables 1 – 3 list all transitions that have been used in the final fit, together with the observed frequencies and the deviations from the calculated ones. All

  1439-4235/01/02/04 $ 17.50+.50/0 CHEMPHYSCHEM **2001**, No. 4

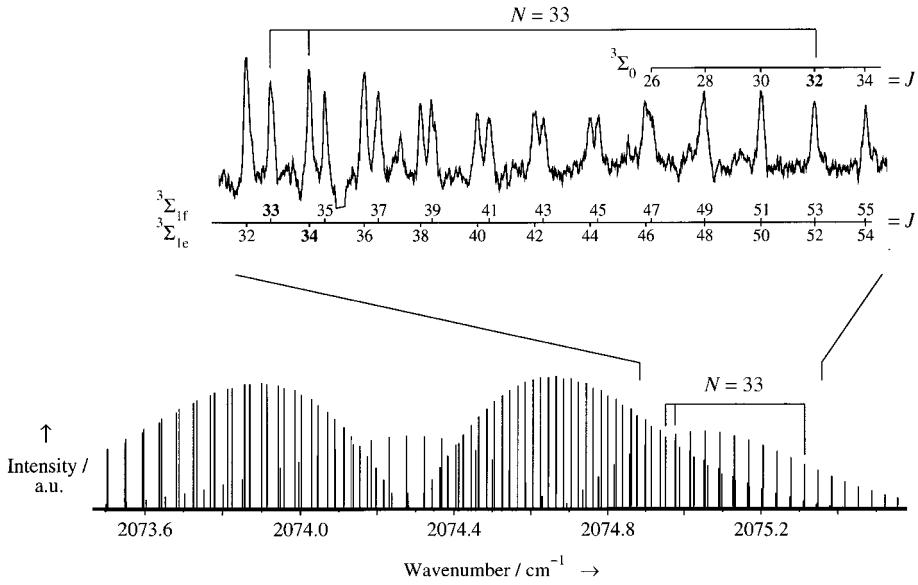

Figure 4. *Stick diagram of the spectrum of linear C_{10} and a portion of the observed spectrum illustrating the large triplet splitting. The Σ_0 band is weaker and shifted to higher frequencies.*

lines are well represented by only nine molecular constants; in order to fit the $^3\Sigma_0$ lines, the centrifugal corrections for the rotation and the spin–spin interaction terms have to be included. The spin–rotation constant γ is close to zero and thus not included in the final fit.

Table 1. *$^3\Sigma_{1e}$ observed line positions [cm^{-1}] of C_{10} in the ν_6 band.*

J	P(J) Obs.	Obs. − Calc.	R(J) Obs.	Obs. − Calc.
2	2074.2388	0.0002	2074.3414	− 0.0007
4	2074.1959	− 0.0010	2074.3833	0.0002
6	2074.1520	− 0.0030	2074.4235	− 0.0005
8	2074.1126	− 0.0004	2074.4657	0.0010
10	2074.0697	− 0.0010	2074.5074	0.0022
12	2074.0279	− 0.0004	2074.5446	− 0.0009
14	2073.9856	0.0000	2074.5865	0.0009
16	2073.9437	0.0009	2074.6251	− 0.0005
18	2073.9015	0.0017	2074.6665	0.0011
20	2073.8566	0.0000	2074.7059	0.0010
22	2073.8130	− 0.0002		
24	2073.7681	− 0.0016	2074.7849	0.0014
26	2073.7257	− 0.0002	2074.8234	0.0009
28	2073.6813	− 0.0007	2074.8623	0.0010
30	2073.6385	0.0007	2074.9010	0.0011
32	2073.5960	0.0025	2074.9380	− 0.0003
34	2073.5494	0.0005	2074.9789	0.0024
36	2073.5043	0.0001	2075.0150	0.0005
38	2073.4583	− 0.0010	2075.0519	− 0.0004
40	2073.4147	0.0005	2075.0896	− 0.0003
42	2073.3695	0.0007	2075.1273	0.0000
44	2073.3235	0.0002	2075.1637	− 0.0009
46	2073.2787	0.0011	2075.2006	− 0.0010
48	2073.2317	− 0.0001	2075.2393	0.0009
50	2073.1855	− 0.0002	2075.2765	0.0015
52	2073.1384	− 0.0010	2075.3121	0.0007
54	2073.0922	− 0.0008	2075.3454	− 0.0023
56			2075.3841	0.0004
58			2075.4202	0.0006
60			2075.4557	0.0005
62			2075.4907	0.0000

The standard deviation of the final fit was $\sigma = 0.00140$ cm^{-1}, which is close to the experimental accuracy of the spectrometer. The obtained molecular parameters are listed in Table 4.

The ground state rotational constant obtained by the present analysis is in excellent agreement with the value $B_e = 0.01046$ cm^{-1} derived from a quantum chemical calculation of the bond lengths.[26] The band origin at 2074.4109(2) cm^{-1} is close to the value of Freivogel et al obtained from a neon matrix.[8] The rotational constant is slightly smaller in the excited state, as expected for a pure stretching mode.

The spin–spin interaction is strong for C_{10}, as indicated by the large value of $|\lambda|$. In contrast to what have been found for C_4 and C_6, the spin–spin coupling constant for C_{10} has a negative sign. The spin–rotation constant γ was not determined from the fit and thus set to zero for upper and lower vibrational state.

In the present study we have assigned the two components of $^3\Sigma_1$ unambiguously. On the other hand, the *J* assignments of the $^3\Sigma_0$ lines are not so certain, because most of the lines are overlapped by the stronger $^3\Sigma_1$ bands. The *J* numbers can be shifted by two or four from the presented ones. The inclusion of the $^3\Sigma_0$ lines in the fit requires additional parameters to be

Table 2. *$^3\Sigma_{1f}$ observed line positions [cm^{-1}] of C_{10} in the ν_6 band.*

J	P(J) Obs.	Obs. − Calc.	R(J) Obs.	Obs. − Calc.
1			2074.3212	− 0.0007
3	2074.2151	− 0.0019	2074.3634	0.0001
5	2074.1730	− 0.0015	2074.4039	− 0.0006
7	2074.1297	− 0.0021	2074.4455	0.0001
9	2074.0889	0.0002	2074.4886	0.0026
11	2074.0452	− 0.0002	2074.5275	0.0012
13	2074.0022	0.0003	2074.5642	− 0.0022
15	2073.9583	0.0003	2074.6047	− 0.0014
17	2073.9179	0.0041	2074.6456	0.0000
19	2073.8692	− 0.0002	2074.6863	0.0015
21	2073.8247	0.0000	2074.7229	− 0.0008
23	2073.7789	− 0.0009	2074.7627	0.0004
25	2073.7344	− 0.0001	2074.8015	0.0009
27	2073.6880	− 0.0011	2074.8374	− 0.0013
29	2073.6446	0.0013	2074.8766	0.0001
31	2073.5960	− 0.0013	2074.9140	− 0.0001
33	2073.5494	− 0.0016	2074.9539	0.0026
35	2073.5043	− 0.0002	2074.9891	0.0007
37	2073.4583	0.0005	2075.0243	− 0.0008
39	2073.4108	0.0000	2075.0597	− 0.0019
41	2073.3642	0.0007	2075.0974	− 0.0004
43	2073.3162	0.0002	2075.1327	− 0.0011
45	2073.2692	0.0009	2075.1688	− 0.0008
47	2073.2210	0.0006	2075.2042	− 0.0009
49	2073.1736	0.0013	2075.2393	− 0.0011
51	2073.1263	0.0024	2075.2765	0.0011
53	2073.0753	− 0.0001	2075.3121	0.0019
55			2075.3454	0.0006

Table 3. $^3\Sigma_0$ *observed line positions [cm^{-1}] of* C_{10} *in the* ν_6 *band.*

Transition	Obs.	Obs. − Calc.	Transition	Obs.	Obs. − Calc.
P(14)	2074.3639	− 0.0034	*R*(20)	2075.0896	− 0.0032
P(12)	2074.4151	0.0030	*R*(22)	2075.1273	− 0.0033
P(10)	2074.4571	0.0007	*R*(24)	2075.1688	0.0008
P(8)	2074.5010	0.0006	*R*(26)	2075.2045	− 0.0005
P(6)	2074.5446	0.0006	*R*(28)	2075.2399	− 0.0017
P(4)	2074.5865	− 0.0007	*R*(30)	2075.2765	− 0.0014
R(8)	2074.8623	0.0044	*R*(32)	2075.3121	− 0.0018
R(10)	2074.9010	0.0029	*R*(36)	2075.3841	− 0.0006
R(12)	2074.9380	0.0002	*R*(38)	2075.4201	0.0005
R(14)	2074.9789	0.0017	*R*(40)	2075.4557	0.0015
R(16)	2075.0150	− 0.0011	*R*(42)	2075.4907	0.0023
R(18)	2075.0519	− 0.0027			

Table 4. Molecular constants [cm^{-1}] of C_{10} *in the* $^3\Sigma_g^-$ *state.*

Parameter	Ground state	$\nu_6 = 1$ State	
G	0.0	2074.4109(2)	2074.5[a]
B	0.0104759(67)	0.0104385(63)	0.01046[b]
D [10^{-9}]	2.45(127)	1.91(120)	
λ	− 1.787(25)[c]	− 1.98340(24)	
λ_D [10^{-5}]	2.27(133)[d]	2.380(48)	

[a] Value obtained from a neon matrix.[8] [b] Ab initio theoretically predicted value.[26] [c] The negative value implies that the $^3\Sigma_1$ states are energetically lower than $^3\Sigma_0$. [d] Derived from the fit to the $^3\Sigma_0$ band. Please note that the electronic spin – rotation constant is negligibly small and has been omitted.

adjusted, λ_D for the ground and excited vibrational state, which otherwise can be ignored. The assignments of the $^3\Sigma_0$ lines given here are based on two criteria, to make a) the standard deviation of the fit to be comparable to the experimental uncertainties and b) the absolute values for λ_D as small as possible.

The obtained spin – spin coupling constant λ is very large and negative for both ground and excited vibrational state. Thus the electronic ground state of C_{10} is an inverted $^3\Sigma$. Since the absolute value of λ is much larger than the rotational constant *B*, the angular momentum coupling case is very close to Hund's coupling case (a), as shown in Figure 2.

The inversion of the $\Omega = 0$ and ± 1 levels indicates that an electronic excited state, very probably a Π state, is not far from the ground state, which pushes the $|\Omega| = 1$ levels selectively downwards. The photoelectron spectroscopy data show that the energy of the lowest excited $^3\Pi$ state is around 1 eV (8000 cm^{-1}) above the ground state for the carbon chain clusters up to C_8.[27] We thus expect for C_{10} the $^3\Pi$ state is still closer to the ground state, which inverts the levels and causes a large λ value. The large vibrational dependence of λ, as well as the large centrifugal correction term for λ, suggests a very small energy separation between the electronic ground state and the perturbing state.

Since the matrix-isolation electron-spin resonance measurements do not give the sign of λ, it is essential to determine the value and the sign of λ for C_8 or C_{12} by high resolution IR spectroscopy. This obviously will be the next target of our carbon cluster project, and has been done for C_8, which will be published in due course.

Experimental Section

Carbon clusters deposited in argon and neon matrices show three stretching modes at 2067.8, 2074.5, and 2081.1 cm^{-1},[8, 19] which have been assigned to the linear carbon clusters C_8, C_{10}, and C_9, respectively. A rotationally resolved gas-phase spectrum of C_9 at 2079.67 cm^{-1} has confirmed the assignment of the 2081.1 cm^{-1} matrix feature.[20] In this paper we have extended the search for C_{10} with high resolution to the 2073 – 2076 cm^{-1} spectral region.

All data have been measured with two separate, but almost identical, tunable diode-laser spectrometers at Cologne and Berkeley. The spectrometers have been described in detail previously.[21, 22] A graphite laser ablation source produces pure carbon clusters of all sizes in a cold supersonic jet of helium. The IR absorption signal was recorded by detecting the light of a tunable IR diode which intersects the cluster jet 20 – 40 times in a Herriott-type multipass optical system. The signals from three HgCdTe photoconducting detectors, the sample, the reference gas (OCS), and the etalon signal for frequency calibration were collected simultaneously and stored with a computer. Signal averaging over 32 – 40 pulses of the ablation source and the use of a bandpass filter have increased the signal-to-noise ratio significantly.

The spectral resolution was better than 10^{-4} cm^{-1} and the absolute frequency accuracy better than 10^{-3} cm^{-1}. The frequency range between 2073 and 2076 cm^{-1} have been recorded without any mode gaps of the tunable diode laser, which covers the whole *P*- and *R*-branch of C_{10} up to $J = 63$.

The authors thank Prof. J. Brown for a fruitful discussion. R.J.S. acknowledges support through an Alexander-von-Humboldt Senior Scientist Award. The Berkeley group is supported by the NASA Astrophysics and NASA Exobiology programs. The Cologne group has been supported by the Deutsche Forschungsgemeinschaft through Research Grant SFB-494 and SFB-301. We kindly acknowledge the Ministry of Science of the Land Nordrhein-Westfalen (Germany), especially D. Dzwonnek, for financial support.

[1] H. W. Kroto, J. R. Heath, S. C. O'Brien, R. F. Curl, R. E. Smalley, *Nature* **1985**, *318*, 162 – 163.
[2] W. Weltner, R. J. Van Zee, *J. Chem. Rev.* **1989**, *89*, 1713 – 1747.
[3] A. Van Orden, R. J. Saykally, *Chem. Rev.* **1998**, *98*, 2313 – 2357.
[4] P. Freivogel, J. Fulara, M. Jakobi, D. Forney, J. P. Maier, *J. Chem. Phys.* **1995**, *103*, 54 – 59.
[5] D. Forney, P. Freivogel, M. Grutter, J. P. Maier, *J. Chem. Phys.* **1996**, *104*, 4954 – 4960.
[6] M. Wyss, M. Grutter, J. P. Maier, *Chem. Phys. Lett.* **1999**, *304*, 35 – 38.
[7] T. Motylewski, O. Vaizert, T. F. Giesen, H. Linnartz, J. P. Maier, *J. Chem. Phys.* **1999**, *111*, 6161 – 6163.
[8] P. Freivogel, M. Grutter, D. Forney, J. P. Maier, *Chem. Phys.* **1997**, *216*, 401 – 406.
[9] S. L. Wang, C. M. L. Rittby, W. R. M. Graham, *J. Chem. Phys.* **1997**, *107*, 7025 – 7033.
[10] S. L. Wang, C. M. L. Rittby, W. R. M. Graham, *J. Chem. Phys.* **1997**, *107*, 6032 – 6037.
[11] W. R. M. Graham, K. I. Dismuke, W. Weltner, Jr., *Astrophys. J.* **1976**, *204*, 301 – 310.
[12] R. J. Van Zee, R. F. Ferrante, K. J. Zeringue, W. Weltner, Jr., *J. Chem. Phys.* **1988**, *88*, 3465 – 3474.
[13] Y. Oshima, Y. Endo, T. Ogata, *J. Chem. Phys.* **1995**, *102*, 1493 – 1500.
[14] T. Ogata, Y. Ohshima, Y. Endo, *J. Am. Chem. Soc.* **1995** *117*, 3593 – 3598.
[15] R. J. Van Zee, G. R. Smith, W. Weltner, Jr., *J. Am Chem. Soc.* **1988** *110*, 609.

[16] J. R. Heath, R. J. Saykally, *J. Chem. Phys.* **1991**, *94*, 3271 – 3272.
[17] N. Moazzen-Ahmadi, J. J. Thong, A. R. McKellar, *J. Chem. Phys.* **1994**, *100*, 4033 – 4038.
[18] H. J. Hwang, A. Van Orden, K. Tanaka, E. W. Kuo, J. R. Heath, R. J. Saykally, *Mol. Phys.* **1993**, *79*, 769 – 776.
[19] G. Monninger, Ph.D. Thesis, Ruprecht-Karl-Universität Heidelberg (Germany), **1995**.
[20] A. Van Orden, R. A. Provencal, F. N. Keutsch, R. J. Saykally, *J. Chem. Phys.* **1996**, *105*, 6111 – 6116.
[21] G. Winnewisser, T. Drascher, T. Giesen, I. Pak, F. Schmülling, R. Schieder, *Spectrochem. Acta A* **1999**, *55*, 2121 – 2142.
[22] T. F. Giesen, A. Van Orden, H. J. Hwang, R. S. Fellers, R. A. Provencal, R. J. Saykally, *Science* **1994**, *265*, 754 – 759.
[23] W. L. Gordy, R. L. Cook, *Microwave Molecular Spectra*, 3rd ed., **1984**, Wiley, New York.
[24] J. M. Brown, J. T. Hougen, K.-P. Huber, J. W. C. Johns, I. Kopp, H. Lefebre-Brion, A. J. Merer, D. A. Ramsay, J. Rostas, R. N. Zare, *J. Mol. Spectrosc.* **1975**, *55*, 500 – 503.
[25] J. B. Tatum, J. K. G. Watson, *Can. J. Phys.* **1971**, *49*, 2693 – 2703.
[26] C. Liang, H. F. Schaefer III, *Chem. Phys. Lett.* **1990**, *169*, 150 – 160.
[27] C. Xu, G. R. Burton, T. R. Taylor, D. M. Neumark, *J. Chem. Phys.* **1997**, *107*, 3248 – 3436.

Received: December 20, 2000 [Z 169]

Multiphoton Excitation of Lanthanides

Joseph R. Lakowicz,*[a] Grzegorz Piszczek,[b] Badri P. Maliwal,[a] and Ignacy Gryczynski[a]

KEYWORDS:

europium · lanthanides · luminescence · multiphoton excitation · terbium

The luminescent properties of the lanthanide ions are of considerable interest to both biochemistry and medical diagnostics. The biochemical interest can be traced to the seminal reviews by Richardson[1] and Horrocks,[2] which described the lanthanides as calcium analogues because of their binding to biomolecules and their preferences for oxygen ligands. There have since been extensive studies of the emission from lanthanides when bound to biomolecules including calcium-binding proteins[3–5] and nucleic acids.[6–8]

The visible absorption and emission spectra of the lanthanides are the result of electronic transitions between the unfilled f-orbitals. These transitions are forbidden, which result in weak absorption of light and long luminescence decay times of 1 – 2 ms. Because the 4f-orbitals are shielded by higher orbitals, the optical transitions are insensitive to the local environment and the luminescent lanthanides are not quenched by dissolved oxygen. Consequently the long decay times persist in oxygenated biological samples. The long decay times of the lanthanides have also have been of value in high sensitivity immunoassays.[9–11] With pulsed excitation, the emission continues after decay of the prompt, interfering autofluorescence from biological samples. The long lived lanthanide emission can be detected at longer times against a completely dark background and result in sensitivities comparable to radioactive detection.

From the above summary, one can see that the lanthanides have extensive biochemical and medical uses. However, an unfortunate result of the millisecond decay times is low molar extinction coefficients of about $0.1\,\text{M}^{-1}\,\text{cm}^{-1}$.[12] Such weak absorption precludes direct excitation of the lanthanides except when using moderately intense laser sources. In medical applications[9–11] and in recent biochemical applications,[13–14] this limitation was overcome by the use of aromatic ligands with good extinction coefficients. These ligands absorb the incident light and transfer the energy to the lanthanides with high efficiency. The chelated lanthanides are not calcium analogues.

Herein, we suggest an alternative approach which allows lanthanides to be used in biochemical systems and in optical microscopy using the red or near infrared (NIR) excitation. The weak absorption of the lanthanides is because the transitions between the f-orbitals are forbidden as a one-photon process. However, the f – f transitions are allowed with two photons.[15–16] We thus considered the use of lanthanide aquo ions with two-photon excitation. Fortunately, the two-photon excitation wavelengths are in the range of 750 – 1000 nm,[15–17] which are now readily available from Ti:sapphire lasers with femtosecond pulse widths. Such lasers are now used routinely in multiphoton spectroscopy and microscopy.[18] Multiphoton excitation (MPE) has the advantages of localized excitation at the optical focal point and minimal photochemical and heating effects due to the low absorption of water.[19–20] We show that two-photon excitation of lanthanides without absorbing chelates can be accomplished with the fundamental output of a Ti:sapphire laser. However, the emission intensities are weak for direct multiphoton excitation of the lanthanides. We also show that lanthanide emission can be sensitized by multiphoton excitation of chelators or proteins to which the lanthanides are bound. The long lifetimes of the lanthanides suggest that two-photon induced emission of lanthanide chelates can be used in multiphoton optical microscopy. However, the weak emission found

[a] *Prof. J. R. Lakowicz, Dr. B. P. Maliwal, Prof. I. Gryczynski*
Center for Fluorescence Spectroscopy
Deptartment of Biochemistry and Molecular Biology
School of Medicine
University of Maryland at Baltimore
725 West Lombard Street
Baltimore, MD 21201 (USA)
Fax: (+1) 410-706-8408
E-mail: cfs@cfs.umbi.umd.edu

[b] *Dr. G. Piszczek*
Institute of Experimental Physics
University of Gdańsk
ul. Wita Stwosza 57
80-952 Gdańsk (Poland)